Agricultural and Forest Meteorology 269–270 (2019) 270–284

Contents lists available at ScienceDirect

Agricultural and Forest Meteorology

journal homepage: www.elsevier.com/locate/agrformet

Integrating potential natural vegetation and habitat suitability into revegetation programs for sustainable ecosystems under future climate change

Shouzhang Peng[a,b], Kailiang Yu[c], Zhi Li[d], Zhongming Wen[a,b], Chao Zhang[a,b,*]

[a] State Key Laboratory of Soil Erosion and Dryland Farming on the Loess Plateau, Northwest A&F University, Yangling 712100, China
[b] Institute of Soil and Water Conservation, Chinese Academy of Sciences and Ministry of Water Resources, Yangling 712100, China
[c] Institute of Integrative Biology, ETH Zürich, Univeritätstrasse 16, Zürich 8006, Switzerland
[d] College of Natural Resources and Environment, Northwest A&F University, Yangling 712100, China

ARTICLE INFO

Keywords:
Potential natural vegetation
Habitat suitability
Land use adjustment
LPJ-GUESS
Yanhe Basin
Revegetation program

ABSTRACT

Global concern about the restoration of vegetation ecosystems has recently increased. Potential natural vegetation (PNV) and climate adaptation concepts should be integrated into revegetation programs to achieve sustainable ecosystems. The Yanhe Basin in the Loess Plateau of China (7687 km^2) has been subjected to intense human activity for centuries. It was selected as the study area because vegetation degradation and restoration are occurring there. The objectives of this study were to (1) evaluate whether the current vegetation pattern is appropriate, and (2) provide a restoration plan for future revegetation programs based on PNV and habitat suitability patterns simulated by the dynamic vegetation model LPJ-GUESS. Current work focused on the parameter calibration and high-resolution climate data of the model over the study area. The comparisons of model performances in the PNV pattern and productivity indicated that parameter calibration was necessary for the model application. PNV of the Yanhe Basin may shift by 21.37–29.67% from 1981–2010 to 2071–2100, mainly in the southern part. Forests may decrease and steppes may increase as the climate becomes drier in the future. Comparisons between an existing land use map and the current PNV pattern indicated that only 40.8% of the forestland was coincident with the current PNV pattern, whereas grassland was a more suitable vegetation type for the rest of the terrain. In contrast, 83.1% of the grassland aligned with the current PNV pattern. Therefore, 16.9% remains to be forested. Current forestland and grassland patterns should be adjusted to cope with future climate change. Broadleaf summer-green shrubs covered a larger area and had higher habitat suitability than forests; they might be the most suitable woody plants for revegetation of the Yanhe Basin. The applied research approach could be extended to other regions undergoing similar revegetation programs and help promote sustainable vegetation management.

1. Introduction

Vegetation restoration can improve degraded terrestrial ecosystems (Crouzeilles et al., 2016). Several restoration programs have been conducted around the world such as the 'Initiative 20 × 20' plan in Latin America and the Caribbean (Crouzeilles et al., 2016), the global Bonn Challenge (Verdone and Seidl, 2017), and the Grain-for-Green Program (GGP) in China (Chen et al., 2015; Li et al., 2017). GGP was the first of these programs to be implemented. Its objective is to mitigate soil erosion through revegetation. The Loess Plateau of China experiences severe water shortages and soil erosion (Feng et al., 2016; Yuan et al., 2015). It was chosen as the site for a pilot GGP trial starting in 1999 and will continue to the middle of the 21st century (Li et al., 2017). Thanks to GGP, soil erosion was effectively controlled in this region. Nevertheless, the vegetation there continues to degrade (Chen et al., 2015) because large-scale conversions of farmland to forestland have depleted soil water (Wang et al., 2015). Therefore, by solving one problem, GGP caused another, primarily because of inadequate

Abbreviations: BSS, broadleaf summer-green shrubs; BST, broadleaf summer-green trees; CRU, climate research unit; GCM, general circulation model; GGP, grain-for-green program; HS, habitat suitability; NET, needleleaf evergreen trees; NPP, net primary productivity; PNV, potential natural vegetation; RCP, representative concentration pathway

* Corresponding author at: No. 26, Xinong Road, Institute of Soil and Water Conservation, Yangling, Shaanxi 712100, China.
E-mail addresses: zhangchaolynn@163.com, szp@nwafu.edu.cn (C. Zhang).

https://doi.org/10.1016/j.agrformet.2019.02.023
Received 17 July 2018; Received in revised form 7 February 2019; Accepted 16 February 2019
Available online 22 February 2019
0168-1923/

vegetation restoration planning (Chen et al., 2015). However, as a result of global climate change, it is difficult to make regional vegetation restoration plans because they need the restored vegetation system to continue functioning in the future. Hence, building sustainable vegetation ecosystems under future climate change is a considerable challenge for global restoration programs. To this end, it is necessary to evaluate the adequacy of the current vegetation pattern and propose a reasonable revegetation plan for the future. Accordingly, a frame of reference aligned with climate change is required to evaluate and restore the vegetation system.

Potential natural vegetation (PNV), considering only the effects of climate, is the last stage of vegetation succession without human activity (Tüxen, 1956). PNV can be used as a frame of reference (Hickler et al., 2012; Somodi et al., 2017; Wang et al., 2013; Zhao et al., 2006). However, Chiarucci et al. (2010) argue that PNV is static and ignores vegetation dynamics. Therefore, they suggested that, in order to accurately describe the dynamic state of mature vegetation, PNV should factor in climate change and vegetation successions. Hence, dynamic PNV may be a more reasonable frame of reference for decision-makers. Planners and managers may intend to locate more suitable environments for vegetation growth to ensure cost-effectiveness of the revegetation programs (Peng et al., 2016). Plant habitat suitability may address this issue (Hirzel and Le Lay, 2008; Peng et al., 2016). The combination of PNV pattern and habitat suitability considering both climate change and vegetation dynamics might provide more detailed information needed for the revegetation programs.

Various species distribution models have been applied to analyze PNV patterns and habitat suitability. These include generalized linear/additive models, maximum entropy models, and tree-based models (Bean et al., 2014; Hirzel and Le Lay, 2008; Merow et al., 2014). They simulated future PNV patterns and habitat suitability under climate change but their facticity has been challenged (Botkin et al., 2007; Pearson and Dawson, 2003) and the assumption of equilibrium between vegetation distribution and climate has been criticized (Svenning and Skov, 2004). Furthermore, they do not account for biotic interactions, the effects of atmospheric CO_2 on plant productivity, terrestrial water cycling, or vegetation successions (Hickler et al., 2012). Therefore, species distribution models support a static PNV concept and do not address the limitations indicated by Chiarucci et al. (2010). Moreover, their habitat suitability determinations are not comparable among different vegetation types. They assume independent relationships between each vegetation type and climate; consequently, they cannot select the most suitable vegetation type for a particular area.

Alternatively, there are process-based dynamic vegetation models like the Lund–Potsdam–Jena Dynamic Global Vegetation Model (LPJ-DGVM) (Sitch et al., 2003), the Lund–Potsdam–Jena General Ecosystem Simulator (LPJ-GUESS) (Smith et al., 2014), and the Spatially Explicit Individual-Based Dynamic Global Vegetation Model (Sato et al., 2007). These account for PNV dynamics (component, succession, productivity, and pattern) under climate and atmospheric CO_2 changes (Hickler et al., 2012; Wolf et al., 2008). They are more effective than species distribution models at interpreting PNV responses to climate change (Pappas et al., 2013). Productivity simulated by dynamic vegetation models represents the total effect of the environment on vegetation, may be comparable among different vegetation types, and could quantify habitat suitability.

Several studies investigated PNV patterns and responses to climate change using dynamic vegetation models (Hickler et al., 2012; Koca et al., 2006; Wolf et al., 2008). However, these studies seldom attempted to evaluate the adequacy of current vegetation patterns. These evaluations could produce practical plans to correct unsuitable vegetation patterns in revegetation programs. Moreover, few studies investigated PNV habitat suitability using dynamic vegetation models. This approach could help develop reasonable and cost-effective restoration plans. It is possible that the low spatial resolution of the PNV projections limited these extended analyses. Most PNV studies using dynamic vegetation models had spatial resolutions ranging from 12 (Hickler et al., 2012) to 55 km (Koca et al., 2006). These distances are insufficient to guide revegetation programs. In addition, these studies often referred to original model parameters, especially the bioclimatic parameters which could determine the PNV patterns, to drive the dynamic vegetation models in different regions (Koca et al., 2006; Smith et al., 2014; Wolf et al., 2008). This may induce a bias in simulating the PNV patterns and then provide imprecise reference for the revegetation programs. Thus, high-resolution inputs and parameter calibrations in the dynamic vegetation models are crucial for revegetation programs.

The aim of this study was to propose a frame of reference to evaluate the adequacy of the current vegetation pattern and to propose plans for revegetation programs based on a dynamic vegetation model. To this end, the focus of this study is on the calibration of model parameters and input of high-resolution climate data at the local scale. Besides, in this study, the focal revegetation region in the Loess Plateau was used as the study area. Specifically, the effects of climate change on PNV patterns and habitat suitability over this region were investigated using the LPJ-GUESS model driven by a climate dataset with high spatial resolution. First, the current PNV patterns and productivities simulated by LPJ-GUESS with original or calibrated parameters were validated by natural vegetation data obtained from field surveys and remote sensing. The validation can illuminate the necessity for calibrating model parameters at a local scale. Then, the effects of climate change on PNV patterns were determined for the vegetation types indigenous to the study area, and the adequacy of the current vegetation pattern was evaluated by matching land use maps with simulated PNV patterns. The output of this analysis can help decision-makers to correct unsuitable land use patterns. Finally, PNV patterns and productivity -based habitat suitability were simulated by the model for each type of woody vegetation. This information may help decision-makers propose reasonable future revegetation plans. The approach used in this study and obtained results should provide guidelines for regions undergoing similar revegetation programs and help develop sustainable vegetation management plans.

2. Material and methods

2.1. Study area

The Yanhe Basin is the focal area of revegetation in the Loess Plateau. It is located in the transitional vegetation zone and is a branch of the Yellow River (36.38°–37.32 °N, 108.65°–110.48 °E) (Fig. 1). It covers an area of 7687 km^2 and is characterized by gullies and hills. Its elevation ranges from 495 to 1795 m. The mean annual precipitation ranges from 424 to 558 mm (Fig. S1). Almost 70% of the annual rain falls between May and September. The mean annual temperature ranges from 6.3 to 12.4 °C in the northwest and southwest, respectively (Fig. S1). Warm temperate deciduous broadleaf and evergreen coniferous forests should occur in the southeast, temperate forest-steppe is expected in the middle, and steppes and desert-steppes should be found in the northwest (Shi et al., 2016). However, due to intensive human activity in the Yanhe Basin over the past centuries, most of the natural vegetation was destroyed and natural landscapes were converted to farmlands. Consequently, there has been a substantial sediment influx into the Yellow River. The GGP launched in 1999 partially restored vegetation and prohibited livestock grazing in the basin. As of 2010, farmland, grassland, and forestland accounted for 43.0%, 45.0%, and 11.2% of the basin, respectively (Fig. 1). These measures effectively controlled soil erosion. Nevertheless, the restored vegetation has already undergone degradation because the GGP considered only topography (slope) rather than climate adaptation (Li et al., 2017).

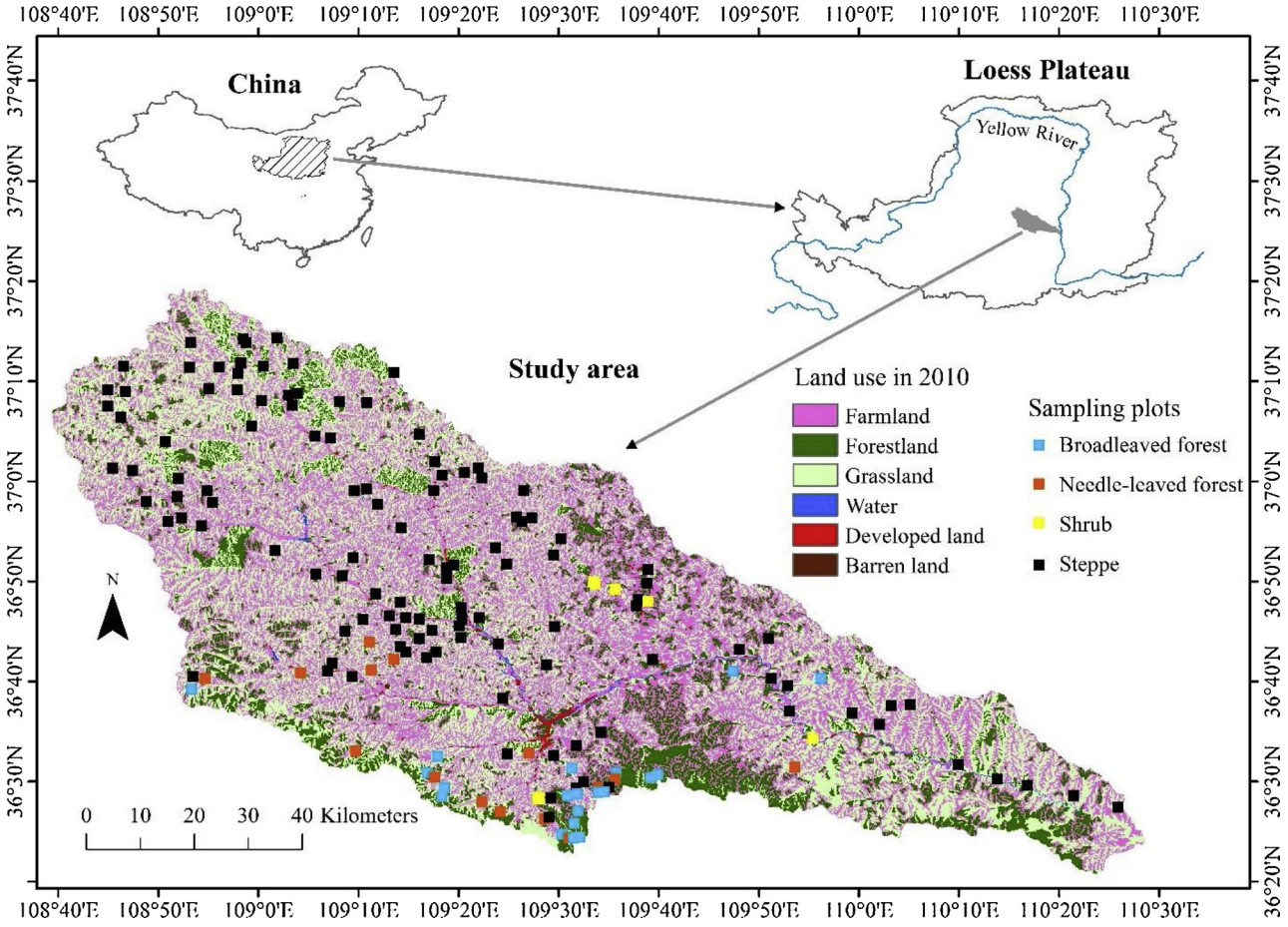

Fig. 1. Land use pattern and vegetation plots investigated across the Yanhe Basin.

2.2. Data collection

2.2.1. Field survey data

A field survey was conducted in 2015–2017 to obtain plant data, calibrate model parameters, and validate simulated PNV patterns. The plot selection criteria included (1) native plant species, (2) absence of human disturbance, and (3) different gradient combinations of temperature and precipitation. One hundred and sixty-five sampling plots were randomly selected including 20 broadleaf forest plots, 15 temperate coniferous forest plots, 7 shrub plots, and 123 grass plots (Fig. 1). The average ages of the sampled trees and shrubs were 110 and 50 yr, respectively, and the grass plots were never grazed. Therefore, the selected plots represented long-term, stable natural regional vegetation.

Location data was recorded for each plot to validate the simulated PNV type. Plant size data and tissue samples were collected from woody plots to determine maximum tree crown area, woody density, and the carbon-to-nitrogen (C:N) mass ratios in fine root and sapwood. Tree crown diameters were measured in eight directions and crown areas were calculated. The maximum tree crown area was determined for each woody plant functional type. Cores were sampled at 1.3 m above the ground from 10–15 trees per plot with an increment borer and stored in paper straws. Fine root samples were also collected. In the laboratory, the weight and volume of each increment core were measured and the density of each woody plant functional type was calculated. Carbon and nitrogen contents were measured in both fine root and sapwood. Thence, the C:N ratios of fine root and sapwood were determined for each woody plant functional type.

2.2.2. Land use maps

The existing land use patterns were obtained from satellite images taken in a previous study (Li et al., 2016) and include two land use maps (2000 and 2010) with a spatial resolution of 100 m. Land use was classified into forestland (including shrubland), farmland, grassland, developed land, water, and barren land (Fig. 1). About 10% of the county field records and photographs in the study area were randomly chosen to assess database accuracy. The six land use classes had accuracies > 94.3% which ensures mapping accuracy on a 100-m scale (Li et al., 2016; Liu et al., 2014). Each land use map was spatially resampled to match the PNV distribution resolution according to the maximum proportion of each land use type in the grid. This approach is commonly used in geographical spatial analysis and provides relatively reliable land use information from high to low resolution (Jong et al., 2013).

2.2.3. Climate, soils, and CO_2 data

PNVs were generated by LPJ-GUESS which, in turn, was driven by monthly climate data, soil texture, and CO_2 concentrations. Monthly precipitation, mean temperature, and cloud cover had a 1-km spatial resolution and covered the period 1951–2100. The data for the period 1951–2014 were downscaled from the Climate Research Unit (CRU) Time Series v. 3.23 dataset at a 0.5° spatial resolution (Harris et al., 2014). Downscaling was performed over the entire Loess Plateau including the Yanhe Basin. Details are described in the supplementary document. The data for the period 2015–2100 were downscaled from general circulation models (GCMs) using representative concentration pathway (RCP) scenarios at a 0.5° resolution (Reclamation, 2013). For the projected data, 28 GCMs were evaluated from surface observations of weather stations according to the mean absolute error (MAE) between the downscaled GCMs and the observed data. The five GCMs with the lowest MAE were selected for this study. These included

CESM1-CAM5 (Neale et al., 2013), NorESM1-M (Bentsen et al., 2013), CSIRO-MK-3-6-0 (Rotstayn et al., 2010), GFDL-ESM2M (Dunne et al., 2012), and GISS-E2-R (Schmidt et al., 2006). The projected cloud cover data were directly downscaled using bilinear interpolation from their respective GCMs. In the present study, the RCP2.6, RCP4.5, and RCP8.5 scenarios were adopted to simulate future PNV and habitat suitability patterns. The mean of the simulation data driven by these five GCMs under one scenario was considered the projected simulation result under this scenario – this assumption might improve future projection reliability (Tebaldi and Knutti, 2007; Weigel et al., 2010).

The soil texture model input was obtained by disaggregating a 0.5° global soil texture from the Food and Agriculture Organization soil dataset (Sitch et al., 2003). Historical CO_2 concentrations for the period 1951–1958 were obtained from McGuire et al. (2001). Those for the period 1959–2014 came from the National Oceanic and Atmospheric Administration (http://www.esrl.noaa.gov/gmd/ccgg/trends/). The CO_2 concentrations under the RCP scenarios for the period 2015–2100 originated from the RCP Database (http://www.iiasa.ac.at/web-apps/tnt/RcpDb).

2.3. Modeling PNV

LPJ-GUESS combines general physiological and biophysical process representations in the popular global model LPJ-DGVM (Sitch et al., 2003) with detailed representation of tree population dynamics, canopy structure, and resource competition in forest gap models (Bugmann, 2001). LPJ-GUESS can be run at different population and community process abstraction levels (Hickler et al., 2012). A complete description is given in Smith et al. (2014). LPJ-GUESS simulates ecosystem dynamics such as species composition, carbon biomass, and net primary productivity (NPP). The PNV type is determined by classifying the carbon biomass according to a set of rules (Wolf et al., 2008).

The model parameters are set according to the major native tree species and plant functional types in an area to obtain the representation of natural vegetation there (Table S1). The plant functional types in the Yanhe Basin are broadleaf summer-green trees (BST), needleleaf evergreen trees (NET), broadleaf summer-green shrubs (BSS), and steppe. Most of model parameters referred to those for similar plant functional types used in a previous study (Smith et al., 2014). Easily-measured parameters like maximum tree crown area, woody density, and the C:N mass ratios of fine root and sapwood were determined in the present study based on the field survey. Bioclimatic parameters like the minimum and maximum survival temperatures in the coldest month and the minimum survival temperature in the warmest month were obtained by spatially overlaying the vegetation distribution and bioclimatic variable patterns. These vegetation and bioclimatic data were obtained from the Scientific Data Center of the Loess Plateau (http://loess.data.ac.cn) (Fig. S2) and the National Ecosystem Observation and Research Network (http://www.cnern.org.cn) (Fig. S3). The former includes the spatial distributions of the typical vegetation types on the Loess Plateau. The vegetation types were identified by remote sensing and field surveys from 1987 to 1990. The latter included mean, minimum, and maximum temperatures for each month from 1961 to 2000. These data were interpolated by surface observations and based on geographical information system technology. Details of these parameters are listed in Table S1.

Simulations began with biomass-free bare ground with fire disturbance and without harvest because grazing and logging are prohibited in the Yanhe Basin. The model was run for 1300 yr until the simulated vegetation and soil carbon were in dynamic equilibrium with the CO_2 and climate from 1951 to 1980. It was then run to simulate carbon biomass for each plant functional type from 1951 to 2100. The model output was the carbon biomass (kg C m^{-2}) per plant functional type and was converted to plant functional type according to the rules in Table 1 (Wolf et al., 2008). To compare existing land use patterns, BST, NET, and BSS were merged to forestland type and the steppe was treated as grassland type (Table 1).

2.4. Modeling habitat suitability

In this study, NPP (kg C m^{-2} yr^{-1}) was used for each plant functional type to quantify its habitat suitability. The mathematical relationship between NPP and habitat suitability (HS) is represented as follows:

$$HS = \frac{NPP - min(NPP)}{\max(NPP) - min(NPP)} \quad (1)$$

where min(NPP) and max(NPP) are the minimum and maximum NPP values, respectively, for one plant functional type within the potential pattern of this plant functional type. HS is in the range 0–1 and represents the effect of habitat on the growth status of this plant functional type. Several studies showed that LPJ-GUESS was highly reliable at simulating the response of vegetation productivity to climate change (Hickler et al., 2012; Wolf et al., 2008). The present study, however, further evaluated the effectiveness of this model at NPP simulation.

In the present study, HS was investigated for each woody plant functional type because they are the focus of the GGP. To ensure completeness of the vegetation system simulation, tree plant functional types treated as simulated objects were included in the initialization file with shrub and grass plant functional types. When one shrub plant functional type was the simulated object, it was included with grass plant functional type in the initialization file. All LPJ-GUESS schemes were run on a high-performance computer platform because many calculations were required to model PNV and HS.

2.5. Evaluating model performance

There was intensive human disturbance in the study area. Consequently, the modeled PNV pattern could not be validated with the existing vegetation map. The present study investigated natural vegetation plots (Fig. 1) to evaluate the current PNV pattern (averaged for the period 1981–2010). Species information was classified as the PNV type used in this study (Table 1). Overall and individual Kappa values were calculated for each PNV type.

In this study, annual NPP based on remote sensing data was used to validate the simulated NPP. The remote sensing NPP had a 500-m spatial resolution and was determined for the period 2001–2013. They were obtained from the MODIS database (Running et al., 2015). The locations of the surveyed plots were noted to match the observed and simulated NPPs. Their NPP values were averaged for the period 2001–2013. Finally, these means were compared for each vegetation type.

2.6. Investigating potential land use adjustment

Land use patterns obtained from the simulated PNV were used to determine potential adjustments. Alignments between the observed and potential natural vegetation were evaluated by overlaying forestland and grassland in the land use map with those of the simulated PNV types. Regions with substantial land use changes in the GGP were examined to identify potential land use pattern adjustments.

3. Results

3.1. Model evaluation

Table 2 presents a comparison of Kappa values for natural vegetation and current PNV types simulated by the original and calibrated parameters. The simulated current PNV type under the calibrated parameters is more consistent with the natural vegetation type than under the original parameters. The overall Kappa value of the former indicates that the PNV pattern simulated by LPJ-GUESS is reasonable.

Table 1
Land cover, model classification, and examples of typical species.

Land cover	Model classification	Typical species
Forestland	BST: > 85% of biomass consists of woody species and 75% of those are BST	*Quercus wutaishanica* Blume, *Populus davidiana*, *Betula platyphylla*
	NET: > 85% of biomass consists of woody species and 75% of those are NET	*Platycladus orientalis* (Linn.) Franco, *Pinus tabuliformis*
	BSS: > 50% of biomass is BSS	*Hippophae rhamnoides* Linn., *Ziziphus jujube*, *Ostryopsis davidiana* Decaisne, *Rosa xanthina* Lindl, *Caragana korshinskii* Kom.
Grassland	Steppe: > 50% of the biomass is this vegetation type	*Thymus mongolicus, Stipa bungeana, Sophora davidii*

Note: BST = broadleaf summer-green trees; NET = needleleaf evergreen trees; BSS = broadleaf summer-green shrubs.

Table 2
Kappa values for modeled PNV and field survey natural vegetation types.

	Kappa for original parameters	Kappa for calibrated parameters
Overall	0.58	0.72
BST	0.61	0.75
NET	0.48	0.63
BSS	0.48	0.65
Steppe	0.62	0.75

Kappa values range from 0 (no fit) to 1 (perfect fit). Kappa > 0.85 = excellent fit; Kappa > 0.7 = very good fit; Kappa > 0.55 = good fit; Kappa > 0.40 = fair fit; Kappa > 0.2 = poor fit (Monserud and Leemans, 1992).

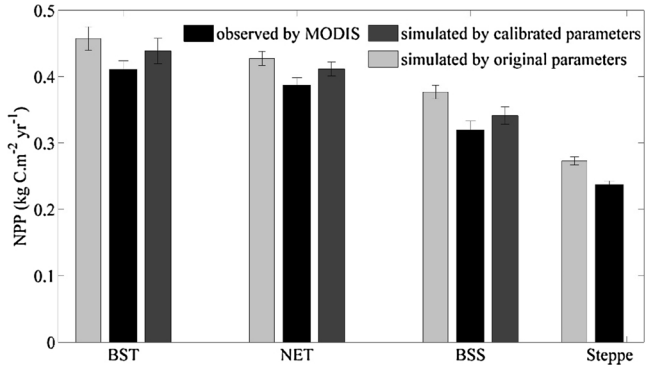

Fig. 2. Comparisons between observed and simulated NPP values (averaged for the period 2001–2013).

Fig. 2 presents a comparison of NPPs based on remote sensing with that simulated by the original and calibrated parameters. The results show that (1) the NPP values simulated by both the original and calibrated parameters were higher than the observed values for each vegetation type, and (2) the NPP values simulated by the calibrated parameters were closer to the observed values for each vegetation type. Therefore, the NPP simulated by LPJ-GUESS is reliable as a variable representing HS. In this study, calibrated parameters were adopted in order to simulate the PNV pattern and HS.

3.2. Spatiotemporal patterns of PNV

The simulations indicated that BST, NET, BSS, and steppes covered 13.31%, 7.26%, 0.03%, and 79.40% of the Yanhe Basin, respectively, from 1981 to 2010 (Table 3). BST and NET were distributed mainly in the southern part of the basin (Fig. 3). The PNV simulation indicated that the spatial distribution and area of each vegetation type may change from 2071 to 2100 (Fig. 3 and Table 3). The area of BST may decrease to 0.63 ± 0.36% under RCP2.6, 0.56 ± 0.12% under RCP4.5, and 5.53 ± 4.13% under RCP8.5. The area of NET may decrease to 0.52 ± 0.31% under RCP2.6 and 1.00 ± 0.80% under RCP4.5, and increase to 9.58 ± 4.21% under RCP8.5. The area of BSS may increase to 0.39 ± 0.13% under RCP2.6, 1.01 ± 0.29% under RCP4.5, and 1.08 ± 0.48% under RCP8.5. The area of steppes may increase to 98.46 ± 0.71% under RCP2.6, 97.43 ± 0.67% under RCP4.5, and 83.81 ± 7.90% under RCP8.5. The latter changes in area were obtained by converting forest to steppe (Table S2). Areas undergoing conversion of vegetation type accounted for 21.37 ± 0.31% under RCP2.6, 21.67 ± 0.24% under RCP4.5, and 29.67 ± 3.57% under RCP8.5. Areas undergoing change in vegetation type were located mainly in the southern part of the study area (Figure S4). Over 74.77 ± 14.18% of each forest type is expected to be converted to steppe.

Table 3
Area percent (%) for each plant functional type during current and future periods.

Plant functional type	1981–2010	2071–2100		
		RCP2.6	RCP4.5	RCP8.5
BST	13.31	0.63 ± 0.36	0.56 ± 0.12	5.53 ± 4.13
NET	7.26	0.52 ± 0.31	1.00 ± 0.80	9.58 ± 4.21
BSS	0.03	0.39 ± 0.13	1.01 ± 0.29	1.08 ± 0.48
Steppe	79.4	98.46 ± 0.71	97.43 ± 0.67	83.81 ± 7.90

3.3. Potential land use adjustment

The land use map for 2010 was overlaid with the current and future PNV maps to reveal differences between observed and simulated land use patterns (Figs. 4 and 5). Only forest and grass were common to both datasets. Therefore, their areas and spatial distributions were compared. The land use map for 2010 indicated that forestland and grassland accounted for 11.2% and 45.0% of the study area, respectively. For the period 1981–2010, the simulated values were 20.6% for forestland and 79.4% for grassland. However, only 40.8% of the observed forestland in 2010 aligned with that of the current simulation map. The PNV type of the remaining 59.1% was grass. Similarly, 83.1% of the observed grassland in 2010 was consistent with that shown in the current simulation map. However, 16.9% of the existing grassland area should be forested. For the period 2071–2100, the simulated forestland values were 1.5 ± 0.7% under RCP2.6, 2.6 ± 0.7% under RCP4.5, and 16.2 ± 7.9% under RCP8.5. The simulated grassland values were 98.5 ± 0.7% under RCP2.6, 97.4 ± 0.7% under RCP4.5, and 83.8 ± 7.9% under RCP8.5. However, the area percentages of observed forestland in 2010 aligning with those in the future simulation maps were only 3.6 ± 1.6% under RCP2.6, 7.0 ± 1.4% under RCP4.5, and 27.4 ± 12.7% under RCP8.5. The PNV type of the remaining forestland should be grass. Similarly, the area percentages of observed grassland in 2010 aligning with those in the future simulation were 98.8 ± 0.7% under RCP2.6, 97.9 ± 0.6% under RCP4.5, and 86.0 ± 7.3% under RCP8.5. The remaining grassland should be forested.

Zones which underwent land use change from 2000 to 2010 were also investigated to determine their suitable PNV types (Fig. 6). Zones showing increases in forestland and grassland were 166 and 101 km^2 in area, respectively. Based on the simulated PNV for this period, grass

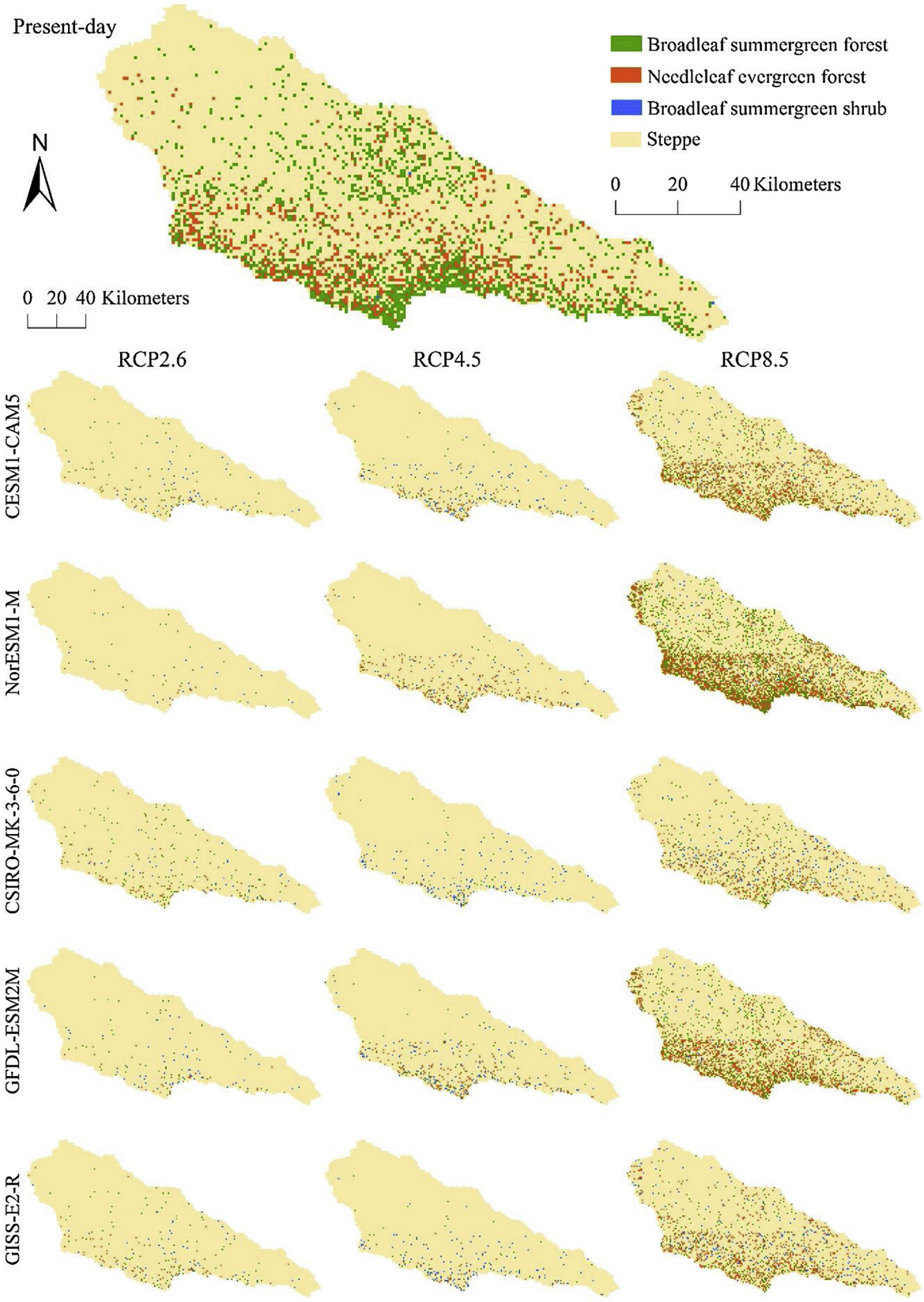

Fig. 3. Present-day (averaged for the period 1981–2010) and future (averaged for the period 2071–2100) PNV patterns.

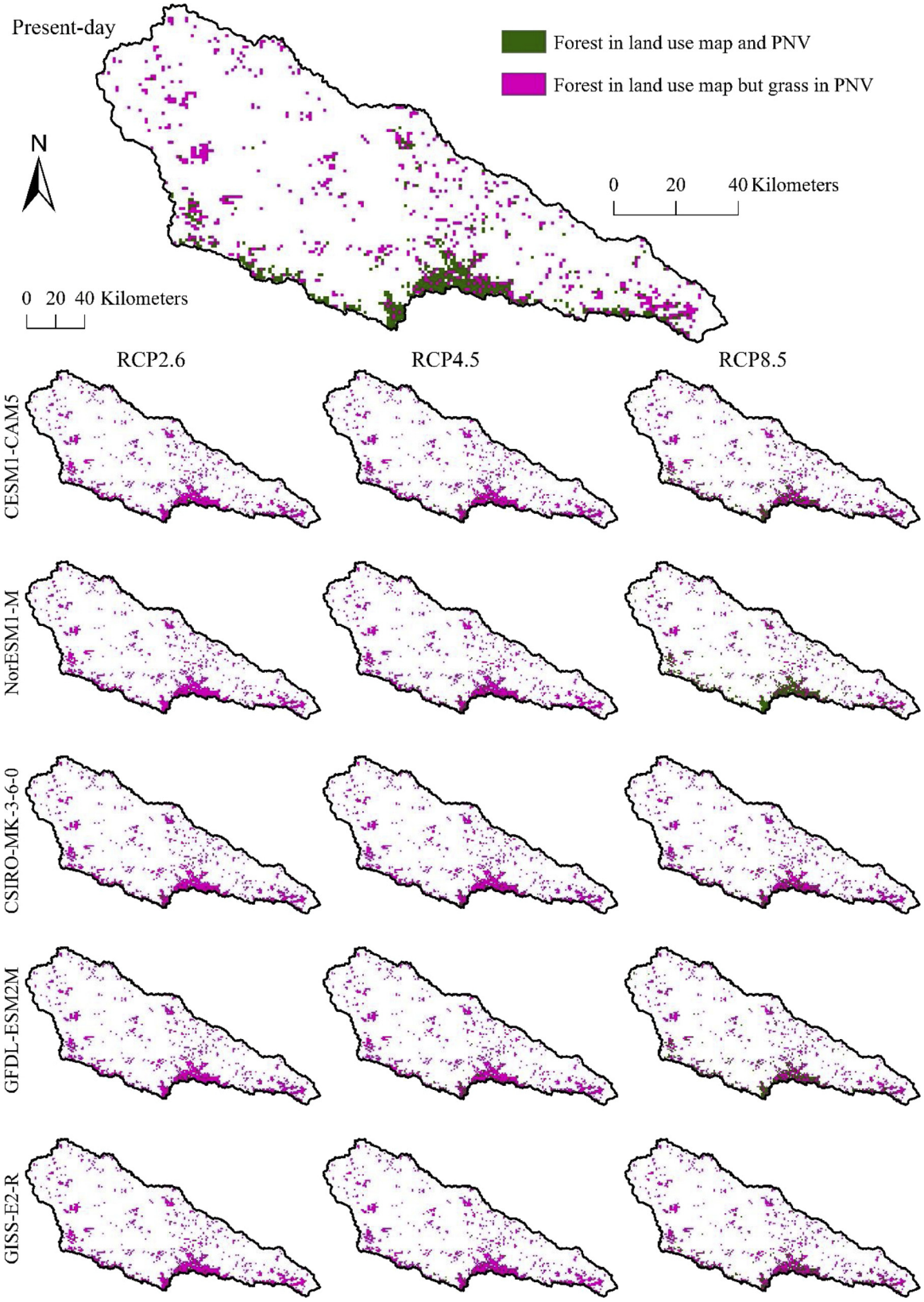

Fig. 4. Spatial overlays of forestland in the 2010 land use map and PNV patterns in current (averaged for the period 1981–2010) and future (averaged for the period 2071–2100) periods.

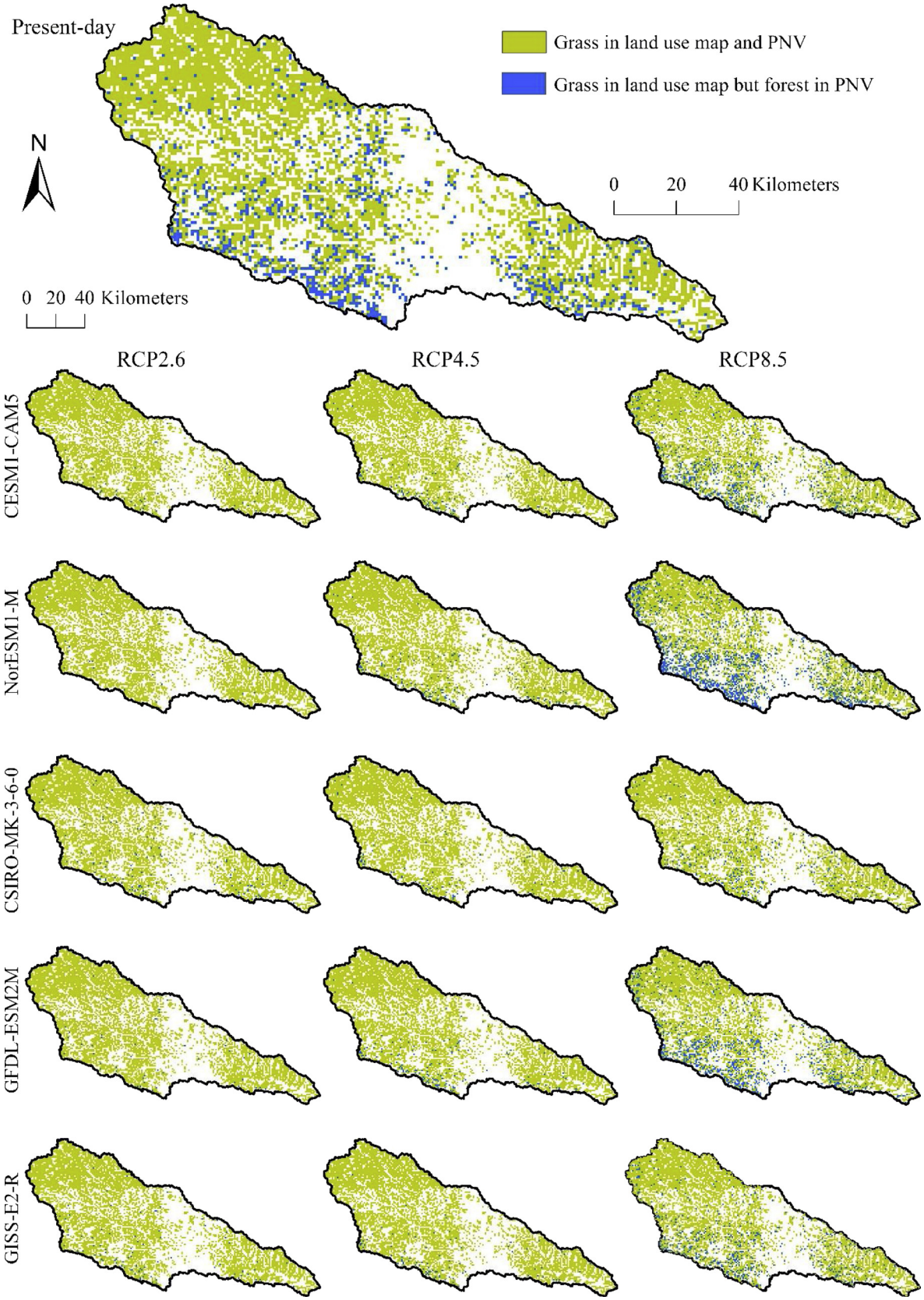

Fig. 5. Spatial overlays of grassland in the 2010 land use map and PNV patterns in current (averaged for the period 1981–2010) and future (averaged for the period 2071–2100) periods.

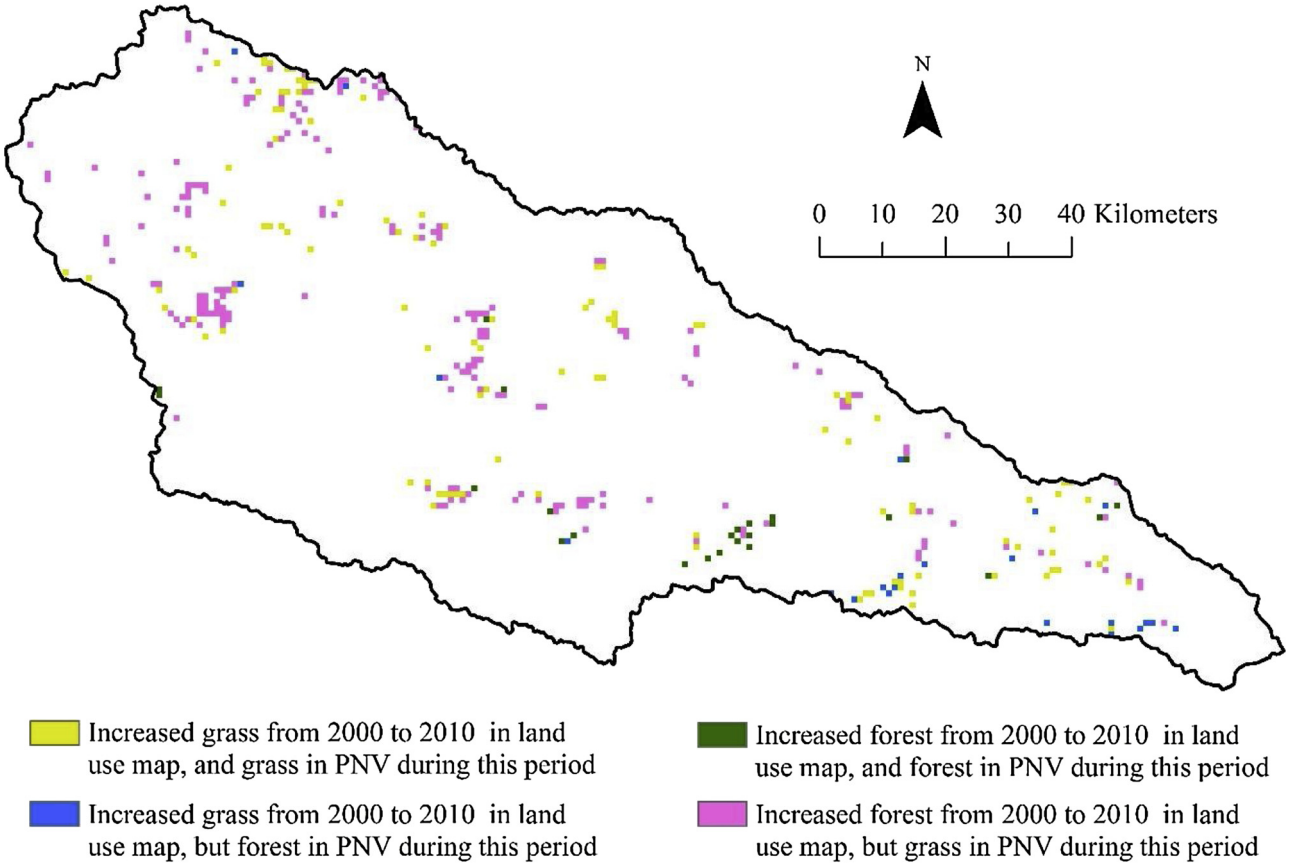

Fig. 6. Spatial overlays between increased forestland/grassland in land use map and PNV pattern from 2000 to 2010.

should account for 89.0% of the zones where forest increased, and forest should account for 17.2% of the zones where grassland increased.

3.4. Spatiotemporal patterns of HS

HS of BST, NET, and BSS in the basin was determined by running the model to simulate NPP for each of these woody plant functional types. Using Eq. (1), HS was quantified for all woody plant functional types in the current and future periods (Figs. 7–9). Maximum and minimum NPP values in Eq. (1) were obtained from all NPP values to compare HS among woody plant functional types.

Compared with the average HS for the period 1981–2010, HS for the period 2071–2100 would decrease for BST, NET, and BSS under RCP2.6, remain the same for BST and NET under RCP4.5, increase for BSS under RCP4.5, and increase for BST, NET, and BSS under RCP8.5 (Table 4). The suitable area would decrease from 33.32% to 1.75 ± 0.81%–25.87 ± 14.77% for BST, from 40.38% to 0.68 ± 0.5%–17.52 ± 11.57% for NET, and from 86.73% to 35.17 ± 10.21%–86.50 ± 15.59% for BSS.

High HS values were calculated mainly for woody plants located in the south part of the basin during both the current and future periods (Figs. 7–9). Comparisons of the HS and area percentages in the same periods revealed that BSS always occupied the highest HS and largest area (Table 4).

4. Discussion

4.1. Interpretation of the results

The results indicate that climate change may significantly affect PNV distribution in the Yanhe Basin. The PNV type in the Yanhe Basin may shift in most areas (21.37 ± 0.31%–29.67 ± 3.57%) between the present day and the end of the 21st century. Areas covered by forest may decrease while steppes may increase (Table 3) because most of the forest may be transformed to steppes (Table S2). This transformation may be the result of the composite effects of temperature and precipitation. Increasing temperature may enhance evapotranspiration by 13–24% during the period 2071–2100 (Peng et al., 2017). However, precipitation may increase by only 6–22% during the same period (Peng et al., 2018). Less precipitation and more evapotranspiration may reduce water availability for plants in the study area by the end of this century. Consequently, the forest area may recede. The advantage of LPJ-GUESS over the species distribution model is that the former accounts for the net interactions between climate change and CO_2 enrichment. Past and future atmospheric CO_2 concentrations were treated as crucial parameters (inputs) driving plant photosynthesis, vegetation response, and PNV patterns in LPJ-GUESS. The projected decreases in forested area were supported by the fact that it is mainly soil moisture which controls vegetation distribution and growth in the study area (Chen et al., 2015; Feng et al., 2016). However, there is ongoing debate regarding the trade-off between CO_2 enrichment and climate change (drought and warming) (Wang et al., 2013). Previous studies reported that even with historical increases in atmospheric CO_2 concentration, woody plants began to decline after 20–30 yr as deep soil moisture receded. These areas transitioned to grass dominance (Chen et al., 2018; Yu and Wang, 2018).

Substantial land use changes over a short time may be unreasonable. Several studies reported low survival and growth rates of woody vegetation planted during the GGP on the Loess Plateau (Cao et al., 2007; Jian et al., 2015) primarily due to unsuitable vegetation type selection (Chen et al., 2015). However, few studies addressed improvement to existing vegetation patterns. This study effectively addressed this issue with simulated PNV. Comparisons between observed land use and simulated PNV indicated that (1) under current climate

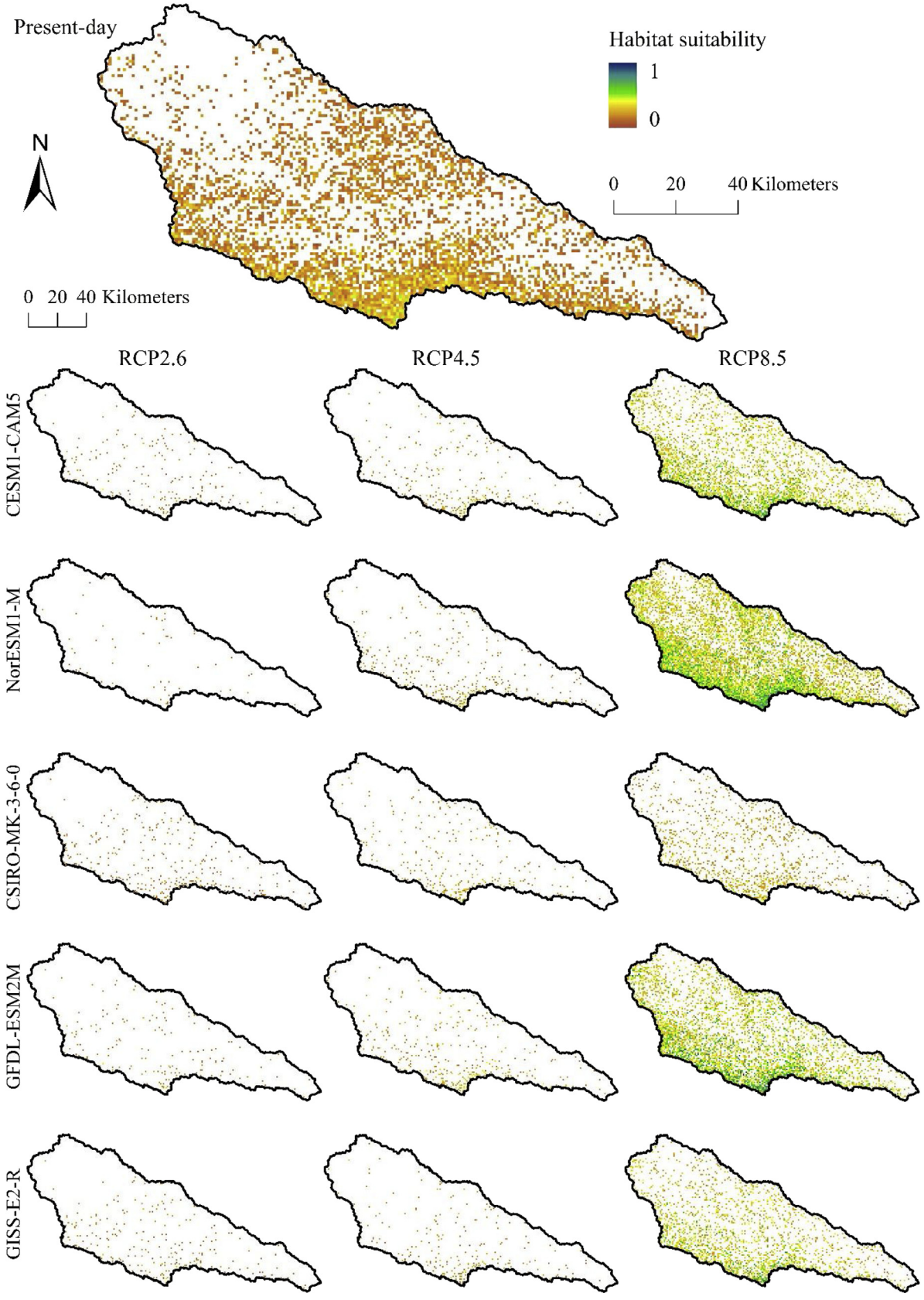

Fig. 7. Modeled present-day (averaged for the period 1981–2010) and future (averaged for the period 2071–2100) HS for broadleaf summer-green trees.

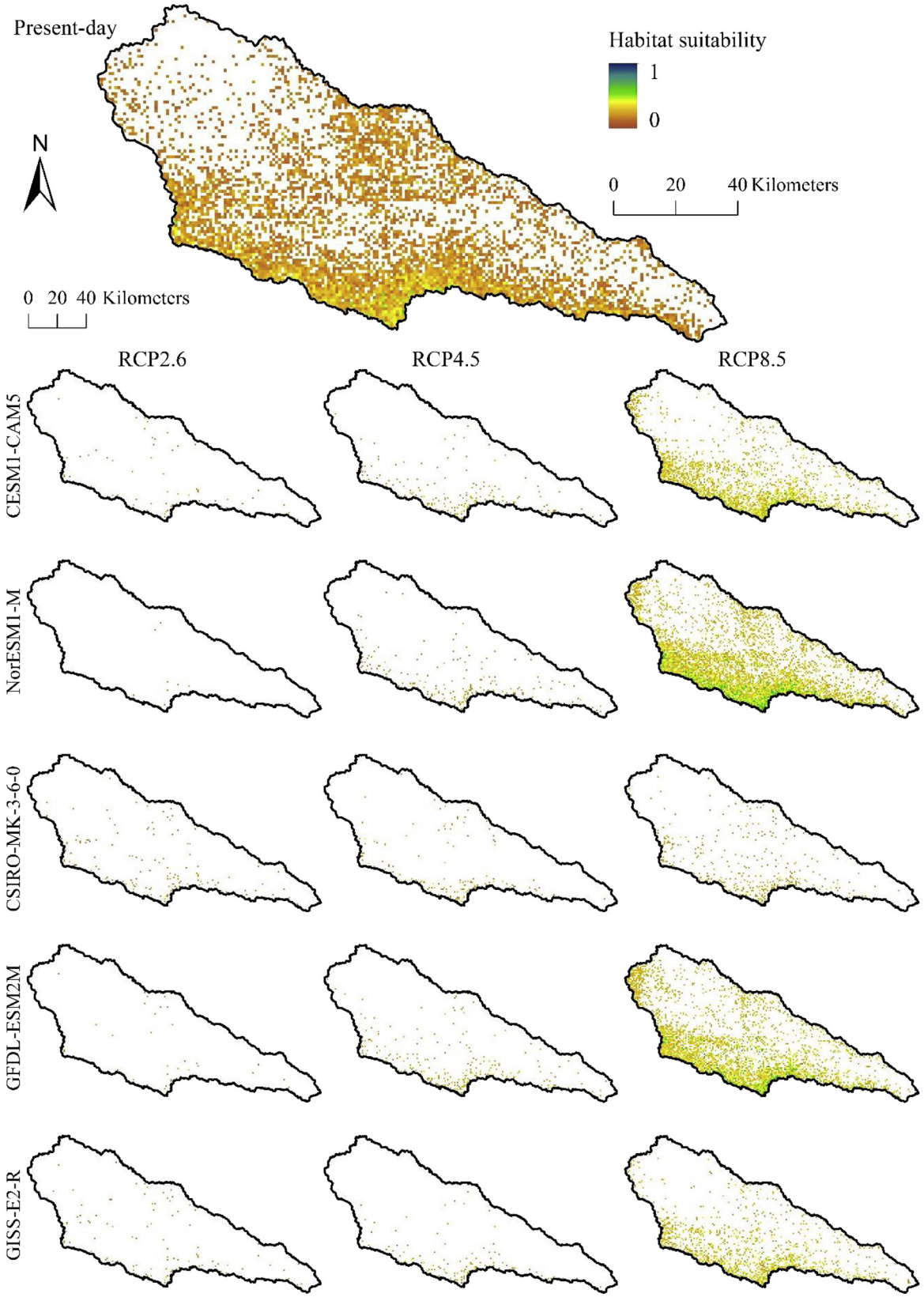

Fig. 8. Modeled present-day (averaged for the period 1981–2010) and future (averaged for the period 2071–2100) HS for needleleaf evergreen trees.

conditions, 59.2% of the existing forestland should be grassland while 16.9% of the grassland should be forested, and (2) under future climate conditions, 72.6 ± 12.7%–96.4 ± 1.6% of the existing forestland should be grassland while 1.2 ± 0.7%–14.0 ± 7.3% of the grassland should be forested (Figs. 4 and 5). Following the GGP, during the period 2000–2010, 89.0% of the increased forestland area should have been grassland and 17.2% of increased grassland area should have been forestland (Fig. 6). This mismatch between observed and simulated

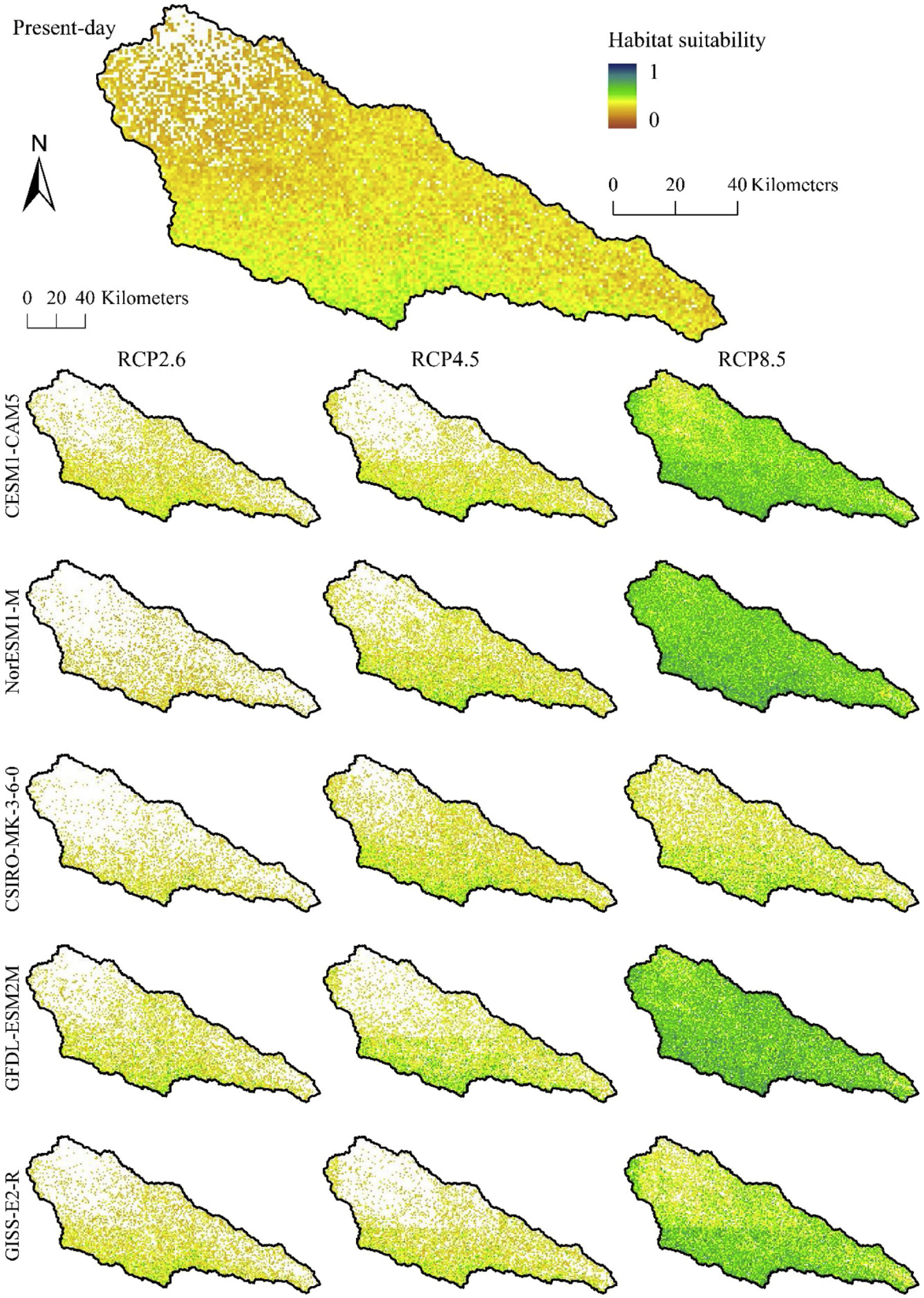

Fig. 9. Modeled present-day (averaged for the period 1981–2010) and future (averaged for the period 2071–2100) HS for broadleaf summer-green shrubs.

land use type underscores the necessity to correct the current land use pattern.

Unlike previous reports, the present study quantified vegetation HS with NPP simulated by LPJ-GUESS. Hirzel and Le Lay (2008) and Bean et al. (2014) reviewed HS studies and suggested that probabilities of species' occurrence based on environmental variables may represent vegetation HS. Peng et al. (2016) determined the HS of a species by considering the amount of environmental resources it utilizes. This

Table 4
Spatial distribution characteristics of HS for BST, NET, and BSS during the current and future periods.

		1981–2010	2071–2100		
			RCP2.6	RCP4.5	RCP8.5
BST	Min	0.01	0.03 ± 0.02	0.04 ± 0.01	0.06 ± 0.02
	Max	0.51	0.34 ± 0.07	0.44 ± 0.07	0.85 ± 0.17
	Mean	0.16	0.12 ± 0.01	0.16 ± 0.02	0.32 ± 0.07
	AP	33.32%	1.75 ± 0.81%	2.77 ± 0.48%	25.87 ± 14.77%
NET	Min	0.07	0.07 ± 0.02	0.08 ± 0.01	0.11 ± 0.04
	Max	0.53	0.26 ± 0.06	0.44 ± 0.06	0.63 ± 0.16
	Mean	0.18	0.14 ± 0.01	0.18 ± 0.02	0.27 ± 0.05
	AP	40.38%	0.68 ± 0.5%	1.72 ± 0.47%	17.52 ± 11.57%
BSS	Min	0.18	0.17 ± 0.01	0.18 ± 0.02	0.22 ± 0.02
	Max	0.54	0.62 ± 0.07	0.69 ± 0.06	0.86 ± 0.05
	Mean	0.32	0.31 ± 0.03	0.35 ± 0.01	0.48 ± 0.07
	AP	86.73%	35.17 ± 10.21%	50.51 ± 7.04%	86.50 ± 15.59%

Note: Min, Max, Mean, and AP are the minimum, maximum, mean, and area percentages, respectively.

evaluation is an application of the ecological niche theory. Previous studies used environmental variables to quantify HS whereas the current study regarded the interaction between environment and vegetation. The authors believe that the HS values generated by the current study are more practical than those reported previously because (1) atmospheric CO_2 and the interaction between environment and vegetation were included; (2) the effect of climate change on HS was reasonably represented; and (3) HS values for the various vegetation types were comparable. The obtained results suggest that climate change may significantly affect the HS of PNV. In dry climates, BSS may cover a larger area (Figs. 7–9) and have higher HS (Table 4) per time period than BST or NET. Therefore, shrub might be preferable for future revegetation programs in the Yanhe Basin. In view of the PNV distribution results, knowing HS patterns may help design more cost-effective and reasonable revegetation plans.

4.2. Uncertainties and caveats

In this study, 1-km spatial resolution climate data were used to explore the effects of climate change. Climate data in current and future periods were downscaled from CRU and GCMs, respectively. The former were generated from surface observations and are highly accurate. The latter are derived from GCMs. GCM-projected data vary among models because of relative differences in model structures, initial boundary conditions, and emission scenarios (Hawkins and Sutton, 2009). Climate data uncertainty is partially reduced by using a multi-model mean. In the present study, the five most suitable GCMs were used out of 28 determined from previous research (Peng et al., 2018), in order to project PNV patterns and HS. These may reduce uncertainty in future simulation results. The projected results indicated that forest may occupy more area and vegetation may have higher suitability under the NorESM1-M with RCP8.5 than those under other GCMs with RCP8.5 (Figs. 3 and 7–9). Future temperature and precipitation under the NorESM1-M with RCP8.5 may be more conducive to plant growth in the study area. Considering the difference in the GCMs, one should use their ensemble mean as the future simulation datum for each RCP scenario.

The dynamic vegetation model may have also introduced uncertainty. LPJ-GUESS simulates ecosystem dynamics at the level of plant functional type rather than the individual. Consequently, there is a gap between simulated PNV at the plant functional type level and vegetation management because decision-makers prefer site-specific plant species over vegetation type simulated by a model. Several constant parameters determine vegetation dynamics and may introduce uncertainty into simulations because plant functional traits may vary with the external environment in the geographic space (Yang et al., 2015). Although this study has not addressed this issue, the calibrated parameters were used to drive the model on the local scale, which could also reduce the uncertainty of model parameters. Furthermore, the comparisons of model performances with original and calibrated parameters indicated that parameter calibration in the local region was crucial for the dynamic vegetation models (Table 2 and Fig. 2). The model does not account for feedback from the vegetation to the climate which may either accentuate or mitigate the impact of climate and, in turn, influence vegetation dynamics (Bonan, 2008). These issues may affect the accuracy of the PNV simulation and introduce uncertainty in revegetation plans. For these reasons, there is a pressing need for a dynamic vegetation model without these limitations (Scheite et al., 2013).

In this study, the land use maps were resampled to a coarse resolution. This process may have introduced uncertainty into calculating the areas of the various land use types. The 1-km resolution used in this study is higher than the spatial resolution in most previous studies. However, a resolution < 1 km should be employed in the future. Land use in the Loess Plateau remains nearly constant on a local (small) scale (Li et al., 2016) so this anomaly probably had a negligible impact on the results.

4.3. Adaptation to climate change for regional revegetation

Climate change may impede future revegetation initiatives. Therefore, factoring in climate change adaptation is necessary (Breed et al., 2013). The Yanhe Basin was selected as a typical area to study regional responses of PNV distribution and HS to climate change. Although the Yanhe Basin was a GGP hotspot, current restoration practices are unreasonable over the long term (Chen et al., 2015) in most areas of the GGP of China (Hua et al., 2016). Our study area spanned both arid and semiarid zones where natural vegetation is abundant. Such regions are typical of most zones implementing the GGP. The detailed vegetation information and downscaled climate data in the present study strongly indicate that the model simulations are reliable and the results are applicable towards fine-scale revegetation programs. Therefore, the authors believe that the Yanhe Basin fairly represented the responses of vegetation dynamics to climate change. The applied research approach may be universally applicable to other regions undergoing similar revegetation programs.

Climate change adaptation strategies may constitute part of the risk management process in sustainable regional revegetation (Dai et al., 2016; Galatowitsch et al., 2009). Several strategies to adapt to/mitigate climate change were developed in earlier studies. These include local-scale planning and implementation, enabling vegetation to respond to change, buffering protected areas, and promoting spontaneous recovery (Bolte et al., 2009; Galatowitsch et al., 2009; Millar et al., 2007). There has been comparatively little research on climate change adaptation for

sustainable revegetation in the Yanhe Basin, Loess Plateau, or even all of China. Only a few proposals were made for regional vegetation restoration in China. That concluded that vegetation types which stabilize the vegetation system should be selected. According to the obtained results, recovery plans should prioritize shrub and grass over forest (Figs. 3 and 7–9). Certain measures should be taken to enable the current land use pattern to adapt to climate change (Figs. 4–6). Vegetation restoration based on HS could be highly cost-effective. According to our data, broadleaf summer-green shrubs might be the preferred woody plant for future revegetation programs in the Yanhe Basin (Figs. 7–9, Table 4). Restoration policies should be revised so that they consider climate adaptations on a local scale. In areas implementing the GGP, vegetation restoration is more closely correlated with topography than climate adaptation (Li et al., 2017). For example, farmland with slopes > 25° should be restored to grassland/forestland (Tang et al., 1998). Therefore, in the future, vegetation restoration policies should integrate topography and climate adaptation.

5. Conclusions

The concern for vegetation ecosystem restoration has increased globally in recent years and integrating PNV and climate adaptation into restoration plans is necessary. In this study, a frame of reference was proposed in order to evaluate the adequacy of current vegetation patterns and to provide restoration plans for revegetation programs based on PNV and HS patterns simulated by a dynamic vegetation model. Furthermore, it was demonstrated that calibrating parameters and employing high-resolution climate datasets in a dynamic vegetation model were crucial for the revegetation programs. Therefore, this study extended PNV towards practical applications. This approach was applied to the Yanhe Basin, China which is undergoing both vegetation degradation and restoration. The method applied in this study enabled the effective evaluation of the current land use pattern, enabled the formulation of a possible correction for it, and provided reasonable restoration plans for the study area. Most forestland in the study area should be transformed to grassland and vice versa. In this way, the vegetation will be compatible with the climate. Moreover, broadleaf summer-green shrubs might be the preferred woody plant in future revegetation programs in the study area. The proposed approach may help mitigate vegetation degradation and provide revegetation plans adapted to climate change in other regions undergoing similar revegetation programs.

Declaration of interest

None.

Acknowledgements

This work was jointly funded by the National Natural Science Foundation of China (Grant No. 41601058), the CAS “Light of West China” Program (Grants No. XAB2015B07 and XAB2017A02), and the Key Cultivation Project of the Chinese Academy of Sciences entitled ‘The promotion and management of ecosystem functions of restored vegetation in Loess Plateau, China’. In addition, the authors wish to thank anonymous reviewers for their constructive suggestions to improve the quality of this article.

Appendix A. Supplementary data

Supplementary material related to this article can be found, in the online version, at doi:https://doi.org/10.1016/j.agrformet.2019.02.023.

References

Bean, W.T., Prugh, L.R., Stafford, R., Butterfield, H.S., Westphal, M., Brashares, J.S., 2014. Species distribution models of an endangered rodent offer conflicting measures of habitat quality at multiple scales. J. Appl. Ecol. 51, 1116–1125.
Bentsen, M., Bethke, I., Debernard, J.B., Iversen, T., Kirkevåg, A., Seland, Ø., Drange, H., Roelandt, C., Seierstad, I.A., Hoose, C., Kristjánsson, J.E., 2013. The norwegian earth system model, NorESM1-M - Part 1: description and basic evaluation of the physical climate. Geosci. Model. Dev. Discuss. 6, 687–720.
Bolte, A., Ammer, C., Löf, M., Madsen, P., Nabuurs, G.-J., Schall, P., Spathelf, P., Rock, J., 2009. Adaptive forest management in central Europe: climate change impacts, strategies and integrative concept. Scand. J. For. Res. 24, 473–482.
Bonan, G.B., 2008. Forests and climate change: forcings, feedbacks, and the climate benefits of forests. Science 320, 1444–1449.
Botkin, D.B., Saxe, H., Araújo, M.B., Betts, R., Bradshaw, R.H.W., Cedhagen, T., Chesson, P., Dawson, T.P., Etterson, J.R., Faith, D.P., Ferrier, S., Guisan, A., Hansen, A.S., Hilbert, D.W., Loehle, C., Margules, C., New, M., Sobel, M.J., Stockwell, D.R.B., 2007. Forecasting the effects of global warming on biodiversity. Bioscience 57, 227–236.
Breed, M.F., Stead, M.G., Ottewell, K.M., Gardner, M.G., Lowe, A.J., 2013. Which provenance and where? Seed sourcing strategies for revegetation in a changing environment. Conserv. Genet. 14, 1–10.
Bugmann, H., 2001. A review of forest gap models. Clim. Change 51, 259–305.
Cao, S., Chen, L., Xu, C., Liu, Z., 2007. Impact of three soil types on afforestation in China’s Loess Plateau: growth and survival of six tree species and their effects on soil properties. Landscape Urban Plan. 83, 208–217.
Chen, Y., Wang, K., Lin, Y., Shi, W., Song, Y., He, X., 2015. Balancing green and grain trade. Nat. Geosci. 8, 739–741.
Chen, N., Jayaprakash, C., Yu, K., Guttal, V., 2018. Rising variability, not slowing down, as a leading indicator of a stochastically driven abrupt transition in a dryland ecosystem. Am. Nat. 191, E1–E14.
Chiarucci, A., Araújo, M.B., Decocq, G., Beierkuhnlein, C., Fernández-Palacios, J.M., 2010. The concept of potential natural vegetation: an epitaph? J. Veg. Sci. 21, 1172–1178.
Crouzeilles, R., Curran, M., Ferreira, M.S., Lindenmayer, D.B., Grelle, C.E.V., Rey Benayas, J.M., 2016. A global meta-analysis on the ecological drivers of forest restoration success. Nat. Commun. 7, 11666.
Dai, E., Wu, Z., Ge, Q., Xi, W., Wang, X., 2016. Predicting the responses of forest distribution and aboveground biomass to climate change under RCP scenarios in southern China. Glob. Change Biol. Bioenergy 22, 3642–3661.
Dunne, J.P., John, J.G., Adcroft, A.J., Griffies, S.M., Hallberg, R.W., Shevliakova, E., Stouffer, R.J., Cooke, W., Dunne, K.A., Harrison, M.J., Krasting, J.P., Malyshev, S.L., Milly, P.C.D., Phillipps, P.J., Sentman, L.T., Samuels, B.L., Spelman, M.J., Winton, M., Wittenberg, A.T., Zadeh, N., 2012. GFDL’s ESM2 global coupled climate–carbon earth system models. Part I: physical formulation and baseline simulation characteristics. J. Climate 25, 6646–6665.
Feng, X., Fu, B., Piao, S., Wang, S., Ciais, P., Zeng, Z., Lü, Y., Zeng, Y., Li, Y., Jiang, X., 2016. Revegetation in China’s Loess Plateau is approaching sustainable water resource limits. Nat. Clim. Change 6, 1019–1022.
Galatowitsch, S., Frelich, L., Phillips-Mao, L., 2009. Regional climate change adaptation strategies for biodiversity conservation in a midcontinental region of North America. Biol. Conserv. 142, 2012–2022.
Harris, I., Jones, P., Osborn, T., Lister, D., 2014. Updated high-resolution grids of monthly climatic observations-the CRU TS3.10 Dataset. Int. J. Climatol. 34, 623–642.
Hawkins, E., Sutton, R., 2009. The potential to narrow uncertainty in regional climate predictions. Bull. Am. Meteorol. Soc. 90, 1095–1107.
Hickler, T., Vohland, K., Feehan, J., Miller, P.A., Smith, B., Costa, L., Giesecke, T., Fronzek, S., Carter, T.R., Cramer, W., Kühn, I., Sykes, M.T., 2012. Projecting the future distribution of European potential natural vegetation zones with a generalized, tree species-based dynamic vegetation model. Glob. Ecol. Biogeogr. 21, 50–63.
Hirzel, A.H., Le Lay, G., 2008. Habitat suitability modelling and niche theory. J. Appl. Ecol. 45, 1372–1381.
Hua, F., Wang, X., Zheng, X., Fisher, B., Wang, L., Zhu, J., Tang, Y., Yu, D.W., Wilcove, D.S., 2016. Opportunities for biodiversity gains under the world’s largest reforestation programme. Nat. Commun. 7, 12717.
Jian, S., Zhao, C., Fang, S., Yu, K., 2015. Effects of different vegetation restoration on soil water storage and water balance in the Chinese Loess Plateau. Agric. Forest. Meteorol. 206, 85–96.
Jong, R., Schaepman, M.E., Furrer, R., Bruin, S., Verburg, P.H., 2013. Spatial relationship between climatologies and changes in global vegetation activity. Glob. Change Biol. Bioenergy 19, 1953–1964.
Koca, D., Smith, B., Sykes, M.T., 2006. Modelling regional climate change effects on potential natural ecosystems in Sweden. Clim. Change 78, 381–406.
Li, J., Li, Z., Lü, Z., 2016. Analysis of spatiotemporal variations in land use on the Loess Plateau of China during 1986–2010. Environ. Earth Sci. 75, 997.
Li, J., Peng, S., Li, Z., 2017. Detecting and attributing vegetation changes on China’s Loess Plateau. Agric. Forest. Meteorol. 247, 260–270.
Liu, J., Kuang, W., Zhang, Z., Xu, X., Qin, Y., Ning, J., Zhou, W., Zhang, S., Li, R., Yan, C., Wu, S., Shi, X., Jiang, N., Yu, D., Pan, X., Chi, W., 2014. Spatiotemporal characteristics, patterns, and causes of land-use changes in China since the late 1980s. J. Geogr. Sci. 24, 195–210.
McGuire, A.D., Sitch, S., Clein, J.S., Dargaville, R., Esser, G., Foley, J., Heimann, M., Joos, F., Kaplan, J., Kicklighter, D.W., Meier, R.A., Melillo, J.M., Moore, B., Prentice, I.C., Ramankutty, N., Reichenau, T., Schloss, A., Tian, H., Williams, L.J., Wittenberg, U., 2001. Carbon balance of the terrestrial biosphere in the Twentieth Century: analyses of CO_2, climate and land use effects with four process-based ecosystem models. Glob.

Biogeochem. Cycles 15, 183–206.
Merow, C., Smith, M.J., Edwards, T.C., Guisan, A., McMahon, S.M., Normand, S., Thuiller, W., Wüest, R.O., Zimmermann, N.E., Elith, J., 2014. What do we gain from simplicity versus complexity in species distribution models? Ecography 37, 1267–1281.
Millar, C.I., Stephenson, N.L., Stephens, S.L., 2007. Climate change and forests of the future: managing in the face of uncertainty. Ecol. Appl. 17, 2145–2151.
Monserud, R.A., Leemans, R., 1992. Comparing global vegetation maps with the Kappa statistic. Ecol. Model. 62, 275–293.
Neale, R.B., Richter, J., Park, S., Lauritzen, P.H., Vavrus, S.J., Rasch, P.J., Zhang, M., 2013. The mean climate of the community atmosphere model (CAM4) in forced SST and fully coupled experiments. J. Climate 26, 5150–5168.
Pappas, C., Fatichi, S., Leuzinger, S., Wolf, A., Burlando, P., 2013. Sensitivity analysis of a process-based ecosystem model: pinpointing parameterization and structural issues. J. Geophys. Res. Biogeosci. 118, 505–528.
Pearson, R.G., Dawson, T.P., 2003. Predicting the impacts of climate change on the distribution of species: are bioclimate envelope models useful? Glob. Ecol. Biogeogr. 12, 361–371.
Peng, S., Zhao, C., Xu, Z., Ashiq, M.W., 2016. Restoration and conservation potential of destroyed Qinghai spruce (Picea crassifolia) forests in the Qilian Mountains of northwest China. Mitig. Adapt. Strateg. Glob. Change 21, 153–165.
Peng, S., Ding, Y., Wen, Z., Chen, Y., Cao, Y., Ren, J., 2017. Spatiotemporal change and trend analysis of potential evapotranspiration over the Loess Plateau of China during 2011–2100. Agric. Forest. Meteorol. 233, 183–194.
Peng, S., Gang, C., Cao, Y., Chen, Y., 2018. Assessment of climate change trends over the Loess Plateau in China from 1901 to 2100. Int. J. Climatol. 38, 2250–2264.
Reclamation, 2013. . Downscaled CMIP3 and CMIP5 Climate and Hydrology Projections: Release of Downscaled CMIP5 Climate Projections, Comparison with Preceding Information, and Summary of User Needs. The U.S. Department of the Interior, Bureau of Reclamation, Technical Services Center, Denver, Colorado, pp. 47.
Rotstayn, L.D., Collier, M.A., Dix, M.R., Feng, Y., Gordon, H.B., O'Farrell, S.P., Smith, I.N., Syktus, J., 2010. Improved simulation of Australian climate and ENSO-related rainfall variability in a global climate model with an interactive aerosol treatment. Int. J. Climatol. 30, 1067–1088.
Running, S., Mu, Q., Zhao, M., 2015. MOD17A3H MODIS/Terra Net Primary Production Yearly L4 Global 500m SIN Grid V006 [Data set]. NASA EOSDIS Land Processes DAAC.
Sato, H., Itoh, A., Kohyama, T., 2007. SEIB–DGVM: a new dynamic global vegetation model using a spatially explicit individual-based approach. Ecol. Model. 200, 279–307.
Scheite, S., Langan, L., Higgins, S.I., 2013. Next-generation dynamic global vegetation models: learning from community ecology. New Phytol. 198, 957–969.
Schmidt, G.A., Ruedy, R., Hansen, J.E., Aleinov, I., Bell, N., Bauer, M., Bauer, S., Cairns, B., Canuto, V., Cheng, Y., Genio, A.D., Faluvegi, G., Friend, A.D., Hall, T.M., Hu, Y., Kelley, M., Kiang, N.Y., Koch, D., Lacis, A.A., Lerner, J., Lo, K.K., Miller, R.L., Nazarenko, L., Oinas, V., Perlwitz, J., Perlwitz, J., Rind, D., Romanou, A., Russell, G.L., Sato, M., Shindell, D.T., Stone, P.H., Sun, S., Tausnev, N., Thresher, D., Yao, M.-S., 2006. Present-day atmospheric simulations using GISS ModelE: comparison to in situ, satellite, and reanalysis data. J. Climate 19, 153–192.
Shi, H., Wen, Z., Paull, D., Jiao, F., 2016. Distribution of natural and planted forests in the Yanhe River catchment: Have we planted trees on the right sites? Forests 7, 258.
Sitch, S., Smith, B., Prentice, I.C., Arneth, A., Bondeau, A., Cramer, W., Kaplan, J.O., Levis, S., Lucht, W., Sykes, M.T., Thonicke, K., Venevsky, S., 2003. Evaluation of ecosystem dynamics, plant geography and terrestrial carbon cycling in the LPJ dynamic global vegetation model. Glob. Change Biol. Bioenergy 9, 161–185.
Smith, B., Wårlind, D., Arneth, A., Hickler, T., Leadley, P., Siltberg, J., Zaehle, S., 2014. Implications of incorporating N cycling and N limitations on primary production in an individual-based dynamic vegetation model. Biogeosciences 11, 2027–2054.
Somodi, I., Molnár, Z., Czúcz, B., Bede-Fazekas, Á., Bölöni, J., Pásztor, L., Laborczi, A., Zimmermann, N.E., 2017. Implementation and application of multiple potential natural vegetation models – a case study of Hungary. J. Veg. Sci. 28, 1260–1269.
Svenning, J.-C., Skov, F., 2004. Limited filling of the potential range in European tree species. Ecol. Lett. 7, 565–573.
Tang, K., Zhang, K., Lei, A., 1998. Critical slope gradient for compulsory abandonment of farmland on the hilly Loess Plateau. Chin. Sci. Bull. 43, 409–412.
Tebaldi, C., Knutti, R., 2007. The use of the multi-model ensemble in probabilistic climate projections. Philos. Trans. Math. Phys. Eng. Sci. 365, 2053–2075.
Tüxen, R., 1956. Die huetige potentielle naturliche Vegetation als Gegestand der Vegetationskarierung. Angewandte Pflanzensozioligie 13, 5–42.
Verdone, M., Seidl, A., 2017. Time, space, place, and the Bonn Challenge global forest restoration target. Restor. Ecol. 25, 903–911.
Wang, H., Prentice, I.C., Ni, J., 2013. Data-based modelling and environmental sensitivity of vegetation in China. Biogeosciences 10, 5817–5830.
Wang, Y., Shao, M., Liu, Z., Zhang, C., 2015. Characteristics of dried soil layers under apple orchards of different ages and their applications in soil water managements on the Loess Plateau of China. Pedosphere 25, 546–554.
Weigel, A.P., Knutti, R., Liniger, M.A., Appenzeller, C., 2010. Risks of model weighting in multimodel climate projections. J. Climate 23, 4175–4191.
Wolf, A., Callaghan, T.V., Larson, K., 2008. Future changes in vegetation and ecosystem function of the Barents Region. Clim. Change 87, 51–73.
Yang, Y., Zhu, Q., Peng, C., Wang, H., Chen, H., 2015. From plant functional types to plant functional traits: a new paradigm in modelling global vegetation dynamics. Progress Phys. Geogr. Earth Environ. 39, 514–535.
Yu, K., Wang, G., 2018. Long-term impacts of shrub plantations in a desert–oasis ecotone: accumulation of soil nutrients, salinity, and development of herbaceour layer. Land Degrad. Dev. 29, 2681–2693.
Yuan, Z., Yu, K., Wang, B., Zhang, W., Zhang, X., Siddique, K.H.M., Stefanova, K., Turner, N.C., Li, F., 2015. Cutting improves the productivity of lucerne-rich stands used in the revegetation of degraded arable land in a semi-arid environment. Sci. Rep. 5, 12130.
Zhao, C., Nan, Z., Cheng, G., Zhang, J., Feng, Z., 2006. GIS-assisted modelling of the spatial distribution of Qinghai spruce (Picea crassifolia) in the Qilian Mountains, northwestern China based on biophysical parameters. Ecol. Model. 191, 487–500.